International Journal of Biological Macromolecules 305 (2025) 141036

Contents lists available at ScienceDirect

International Journal of Biological Macromolecules

journal homepage: www.elsevier.com/locate/ijbiomac

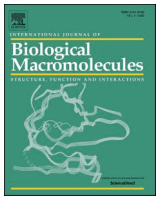

Development of a two-probe competitive enzyme-linked immunosorbent assay for porcine epidemic diarrhea virus based on magnetic nanoparticles

Junru Sun [a,b,1], Ruiqin Zhu [a,b,1], Mengxiang Wang [a,b], Jinxing Song [c], Lei Zhou [a,b], Zhuoya Sun [a,b], Yanze Li [a,b], Liuyang Jiao [a,b], Lu Xia [a,b], Hua He [a,b], Gaiping Zhang [a,b,d,*], Yanan Wu [a,b,*]

[a] International Joint Research Center of National Animal Immunology, College of Veterinary Medicine, Henan Agricultural University, Zhengzhou 450046, China
[b] Ministry of Education Key Laboratory for Animal Pathogens and Biosafety, College of Veterinary Medicine, Henan Agricultural University, Zhengzhou 450046, China
[c] College of Veterinary Medicine, Henan University of Animal Husbandry and Economy, Zhengzhou 450046, China
[d] Longhu Laboratory, Zhengzhou 450046, China

ARTICLE INFO

Keywords:
Porcine epidemic diarrhea virus
Magnetic nanoparticles
N protein
Two-probe competitive ELISA

ABSTRACT

Porcine epidemic diarrhea (PED) causes significant economic losses to the pig farming industry worldwide and currently lacks an effective vaccine. Multiple detection assays and protein purification methods use magnetic nanoparticles due to their biocompatibility, high specific surface area, and solution suspension properties. In this study, a two-probe competitive ELISA based on magnetic nanoparticles for detecting PEDV N protein was developed. MNPs-N and McAb-HRP probes were prepared and the procedure was optimized to identify the ideal reaction conditions. Compared to other methods, the developed method shortens the detection time to 50 min. The coefficient of variation (CV) for intra- and inter-lot replicates was less than 10 %, with reproducibility. The coincidence rate with commercial kits is 93.07 %, making this method reliable and suitable for PED immune monitoring and diagnostics.

1. Introduction

Porcine epidemic diarrhea virus (PEDV) causes porcine epidemic diarrhea (PED) [1]. It is acute and highly contagious, with clinical manifestations like vomiting, diarrhea, and dehydration [2]. PEDV affects pigs of all ages, but piglets have high mortality rates [3,4]. First identified in the United Kingdom in 1971, [5] the disease rapidly spread across Europe by 1976, causing significant economic losses [6]. Since the 1980s, PEDV has also spread in Asia [7]. The vaccine strain CV777 provided immunity, but as mutated strains emerged in 2010, the virus affected even those previously vaccinated. PED ranks among the most devastating epidemics in the swine industry [8–10]. Piglet mortality due to PEDV infection can reach 20 %–30 %, impacting China's pig industry severely [11,12]. Given the global prevalence and substantial economic impact, developing effective vaccines against PEDV is a priority [13].

PEDV encodes four structural proteins; namely N, S, M, and E protein [14]. Studies indicate that PEDV can co-infect with porcine coronaviruses like PDCoV, and TGEV. But even with other proteins, detection of viral particles requires PEDV N protein [15]. The N protein, or nucleocapsid protein, constitutes a significant portion of the viral proteins and exhibits high sequence conservation [16]. This makes it an ideal target for diagnostic tools with high sensitivity and specificity, facilitating early detection and accurate diagnosis of PED [17].

Magnetic nanoparticles (MNPs), also called magnetic microspheres, are a significant research topic in nanomaterial science [18]. They can be quickly separated from liquids using magnetic fields and reused [19]. Their biocompatibility, large surface area, stability, and solution suspension properties [20] make MNPs ideal in drug delivery mechanisms [21,22], pharmaceuticals [23], separation and purification processes [24], and wastewater treatment [25,26]. Current research shows potential beyond these fields, extending to MRI contrast agents [27], green catalysts [28,29], cell labeling [30], controlled drug release [31], and protein separation. MNPs can be categorized into organic and inorganic particles [32]. Organic MNPs are composed of magnetic materials

* Corresponding authors at: International Joint Research Center of National Animal Immunology, College of Veterinary Medicine, Henan Agricultural University, Zhengzhou 450046, China.
E-mail addresses: zhanggaip@126.com (G. Zhang), wlyananjiayou@yeah.net (Y. Wu).
[1] These authors contributed equally to this work.

https://doi.org/10.1016/j.ijbiomac.2025.141036
Received 26 November 2024; Received in revised form 12 February 2025; Accepted 12 February 2025
Available online 17 February 2025

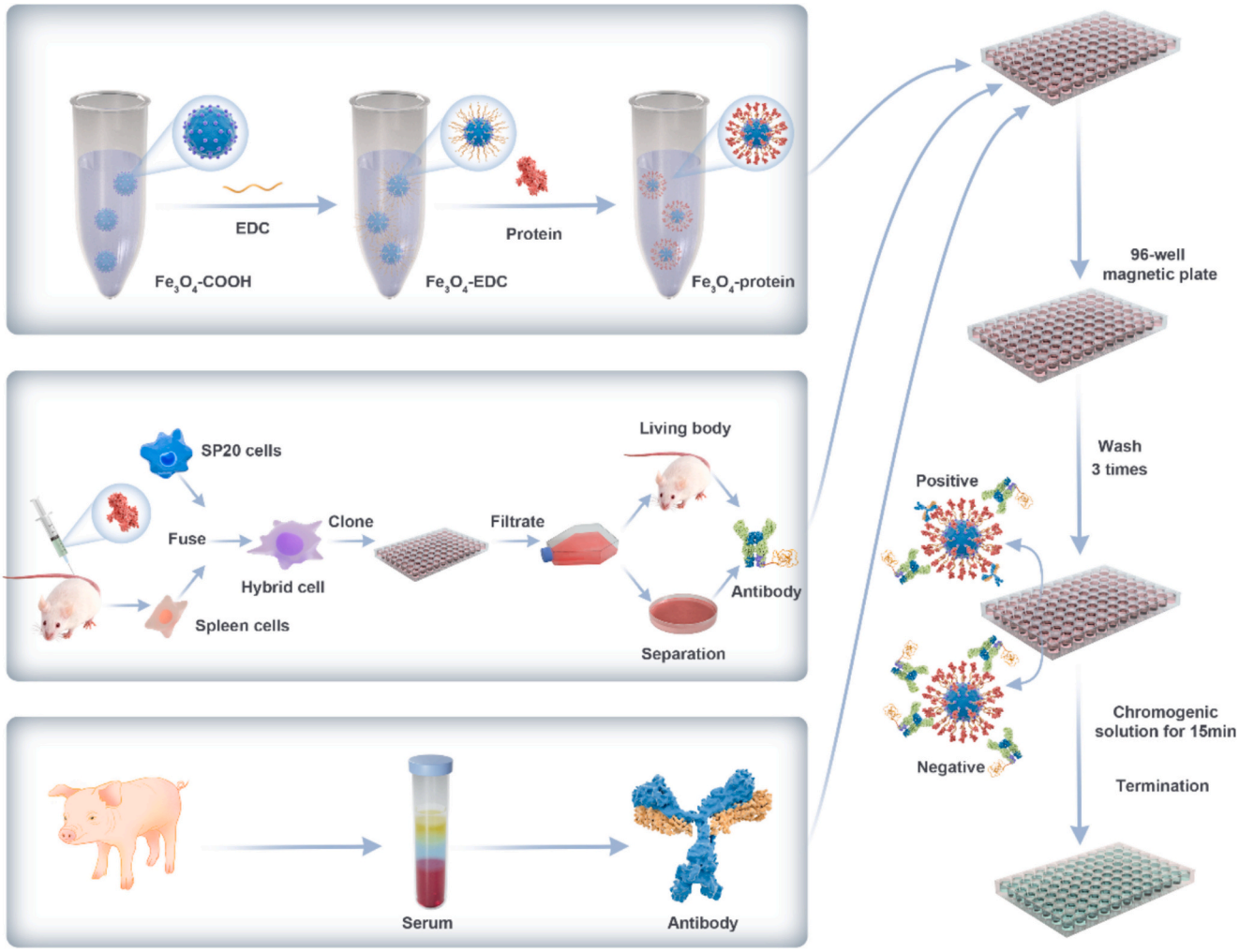

Fig. 1. Schematic representation of the two-probe competitive ELISA technique.

combined with natural or synthetic polymers. They are preferred for *in vivo* drug delivery due to their biocompatibility and degradability [33]. Inorganic MNPs are made from iron, iron oxides, or other metals with inorganic materials. Various types exist, with Fe_3O_4 magnetic microspheres being the most common. In this study, Fe_3O_4 magnetic microspheres were used, owing to their advantages of external magnetic field responsiveness, and high thermal and chemical stability, facilitating broader applications [34].

An MNPs-based two-probe competitive enzyme-linked immunosorbent assay (ELISA) was developed to detect anti-PEDV N protein antibodies. Monoclonal antibodies were generated by immunizing mice with the N protein. These were conjugated with MNPs to prepare MNPs-N probes. The sodium periodate method was used to prepare McAb-HRP probes. Further optimization led to the successful development of the two-probe competitive ELISA. Results obtainable in 50 min, excellent inter- and intra-batch reproducibility, and potential for PED immunosurveillance, make this method significant in PED prevention and control.

MNPs were converted into MNPs-N probes by coupling their carboxyl groups with the amino groups of N protein. The HRP-McAb probe was generated by labeling monoclonal antibodies (McAb) with horseradish peroxidase (HRP). HRP-McAb competitively binds to MNPs-N with the antibodies from the sample. MNPs have dispersing and suspending properties; hence, MNPs-N can be suspended, reducing the distance between antibodies, and accelerating the formation of MNPS-N antibodies. The antigen-antibody competition reaction is expedited and more sensitive compared to traditional methods. This principle is illustrated in Fig. 1.

2. Experiment

2.1. Materials and reagents

RPMI-1640 medium and Dulbecco's modified Eagle's medium (DMEM) were procured from Shanghai Yuanpei Biotechnology Co., LTD. (Shanghai, China). N-hydroxythiosuccinimide sodium salt (NHC) and N-(3-Dimethylaminopropyl)-N′-ethylcarbodiimide hydrochloride (EDC) were procured from Shanghai Aladdin Biochemical Science and Technology Co. Ltd. (Shanghai, China). EDC activates MNPs carboxyl group, and NHC is a catalyst. Immunologic adjuvants were purchased from Biodragon (Suzhou, China). The 96-well magnetic labeling plate was purchased from Nanjing Dongna Biotechnology Co. (Nanjing, China). Morpholine ethanesulfonic acid (MES) was purchased from Merck Millipore (Billerica, MA, USA). Horseradish Peroxidase (HRP) was purchased from Sigma-Aldrich (St. Louis, MO, USA).

2.2. Serum samples

Positive standard sera for ASFV and pseudorabies virus (PRV) were procured from the China Veterinary Culture Collection Center (CVCC, Beijing, China). Positive serum samples for porcine reproductive and respiratory syndrome virus (PRRSV) and clinical serum samples were

pre-collected and preserved.

2.3. Synthesis and characterization of MNPs-N

The methodological framework outlined in the preceding publication was followed [35]. 2 mg MNPs (10 mg/mL) were withdrawn, magnetically separated, washed with MES (0.015 M, pH = 5.5) solution twice, and resuspended. 0.2 mg EDC (10 mg/mL) and NHC (10 mg/mL) were added, and the solution was stirred for 30 min at room temperature. The mixture was magnetically separated, and the supernatant was discarded. The MNPs were washed with MES solution and resuspended. Of N protein, 40 μg was added, and the solution was incubated, stirring, for 4 h at room temperature. The solution was magnetically separated and washed with PBST buffer (pH = 7.4) twice. The supernatant was retained to detect the coupling efficiency of the MNPs and N protein. The unbound sites on MNPs were blocked by adding 1 % BSA (PBST as solvent) and the solution was stirred for 1 h at room temperature. MNPs-N was washed with PBST buffer, resuspended with 0.2 mL of PBST buffer, and stored at 4 °C.

Transmission electron microscopy and laser particle size analyzer were used to characterize MNPs-N synthesis.

2.4. Screening and characterization of anti-N protein monoclonal antibodies

30 μL (1 μg/μL) of purified N protein was emulsified with 30 μL of QuickAntibody-Mouse 5 W Lactic Acid Water Adjuvant to immunize two 6-week-old BALB/c female mice intramuscularly. Mice antibody production was monitored using ELISA. The mouse having higher antibody levels was euthanized, and its spleen was ground and fused with SP2/0 cells. These hybridoma cells were screened by indirect ELISA for positive results and subsequently subcloned thrice using limited dilution. Cells secreting N protein-specific antibodies were expanded and cultured to make ascites and were purified using a Protein G affinity chromatography column.

Western blotting (WB) was used to assess the reactivity of the monoclonal antibody against the N protein. The N protein sample was mixed with 6× sample buffer, boiled, and separated using 10 % SDS-PAGE. The proteins were then transferred to a PVDF membrane, blocked with 5 % skim milk in PBST. A hybridoma supernatant was prepared as the primary antibody, and an enzyme-labeled goat anti-mouse antibody as the secondary antibody.

Immunofluorescence assay (IFA) was used to assess the reactivity of the monoclonal antibody against the N protein. Vero cells cultured in 24-well plates were inoculated with PEDV and monitored every 12 h until lesions developed. Upon detecting lesions, the culture medium was washed with PBS thrice. The cells were fixed in paraformaldehyde for 30 min and then washed with PBS. 0.1 % Triton X-100 was added and kept for 15 min at room temperature to permeabilize the cells. After discarding the solution, the cells were rinsed with PBS thrice. The solution was blocked with 5 % BSA for 1 h at room temperature. The blocking solution was discarded, and the wells were washed with PBS thrice. The hybridoma supernatant was added to each well and incubated for 1 h at room temperature. The wells were washed with PBS and then diluted with fluorescein isothiocyanate (FITC)-labeled goat anti-mouse IgG (1:500) and incubated for 1 h at room temperature in the dark. The wells were washed with PBS, and the samples were stained with DAPI for 30 min. The stain was discarded, and the samples were rinsed with water and PBS, thrice each. The stained cells were observed under a fluorescence microscope.

Monoclonal antibody isoforms were determined using a mouse monoclonal antibody isoform kit.

2.5. Synthesis and characterization of McAb-HRP probes

Previously published steps were followed. [36]: 5 mg of HRP was dissolved in 1 mL of water to make the final concentration 5 mg/mL, and 200 μL of 0.1 M $NaIO_4$ was added. This was stirred continuously and incubated for 20–30 min, in the dark, at room temperature. The solution was poured into a dialysis bag (8000–14,000 D molecular weight cut-off), and dialyzed in 1 mM sodium acetate buffer (pH = 4.4) for 12 h at 4 °C. 200 μL of 0.2 M (pH = 9.6) borate buffer was added to the dialysate, and the pH was adjusted to 9.5 by adding 1 M NaOH, and 10 mg of purified antibody (4 mg/mL in PBS). This mixture was gently stirred for 12–16 h at 4 °C. 235 μL of freshly prepared 4 mg/mL $NaBH_4$ solution was added (47 μL NaBH4 per 1 mg HRP), mixed well, and kept for 2 h at 4 °C. An equal volume of saturated ammonium sulfate solution was added to precipitate the purified antibody. The solution was kept for 30 min at 4 °C, then centrifuged at 12000 r/min for 30 min at 4 °C. The supernatant was discarded, the precipitate was resuspended in PBS, and the resuspension was dialyzed for 12–16 h in PBS at 4 °C. The dialyzed solution was centrifuged at 12000 r/min for 10 min, and the supernatant was stored at −80 °C. This was used to label the antibodies.

The absorption peak of the McAb-HRP probe was detected using a UV spectrophotometer, and the McAb-HRP probe was characterized by direct ELISA.

2.6. Competitive ELISA procedure

5 % BSA solution (200 μL) was added to each well, and the plate was incubated for 1 h at 37 °C. The plate was patted dry and stored at 4 °C. 50 μL each of MNPs-N and McAb-HRP probes were added to each well. Either 50 μL of PEDV-positive serum or the test sample was added, with PBS as a blank control. The plate was gently shaken and then allowed to stand for 30 min at room temperature. The plate was then transferred onto a 96-well magnetic plate, and the solution was magnetically separated for 10 s. The supernatant was discarded, and the plate was washed four times with PBST buffer. 100 μL of color development solution was added and left at room temperature. 50 μL of reaction termination solution was then added. The absorbance was measured at 450 nm, using PBS as a control. The percent inhibition (PI) was calculated using the formula: $PI = \left(1 - \frac{OD_{450\ nm}\ positive\ value\ (P)}{negative\ value\ (N)}\right) \times 100\%$.

2.7. Optimization of competitive ELISA conditions

The optimal concentration of MNPs-N and the dilution of McAb-HRP probes were determined using the checkerboard method. MNPs-N probe concentrations ranged from 0.2 μg/mL to 8 μg/mL in PBS, while McAb-HRP probe dilutions ranged from 1:500 to 1:8000. After establishing binding sites, 50 μL of MNPs-N probe was added vertically to the plate, while 50 μL of McAb-HRP probe, horizontally. The remaining steps were the same as in Section 2.5. The optimal concentrations and dilutions were based on observed OD values.

Positive sera were diluted with PBS at various ratios (undiluted, 1:1, 1:2, 1:5, 1:10, and 1:20). Equal volumes of MNPs-N and McAb-HRP probe were mixed in each dilution. The mixtures were incubated for 30 min at room temperature. The subsequent steps were executed as previously described. The best serum dilution was the one yielding the highest PI value (1-$OD_{450\ nm}$ positive/negative value).

Based on the optimized conditions for MNPs-N probe concentration, McAb-HRP probe dilution, and serum dilution, the optimal reaction time was determined. ELISA assays were conducted at room temperature with reaction times ranging from 5 to 35 min. To determine the optimal color development time, TMB solution was added, and the reactions were incubated in the dark for up to 25 min, before adding the termination solution. Absorbance was measured at 450 nm using a multifunctional enzyme marker.

2.8. Criteria for determining positivity and negativity

To establish critical values, 30 PEDV-negative sera were tested using

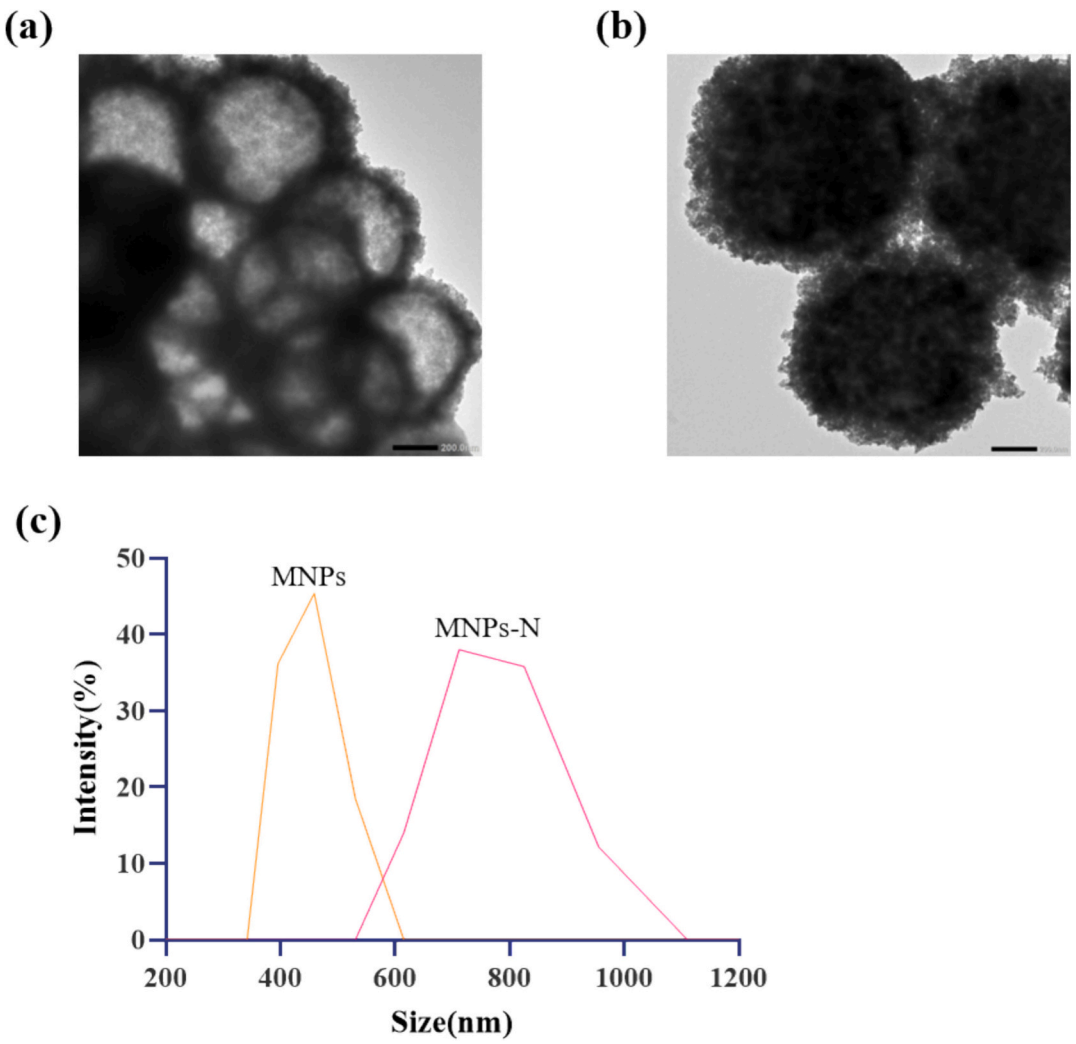

Fig. 2. Characterization of MNPs and MNPs-N. (a) Representative TEM images of MNPs. (b) Representative TEM image of MNPs-N probe. (c) Particle size distribution of MNPs and MNPs-N.

competitive ELISA, using the optimized conditions. The PI values were computed, and the average inhibition rate (X) and standard deviation (SD) of the samples were calculated. A sample's PI value was deemed negative if PI $\leq$ X + 2SD, and positive if PI $\geq$ X + 3SD.

2.9. Repeatability and specificity assessment

Seven sera samples were selected for the assay to calculate inter- and intra-batch coefficients of variation (CV = standard deviation (SD)/ mean × 100 %). This assessed the reproducibility of the competitive ELISA.

PRRSV-positive, PRV-positive, PDCoV- positive and ASFV-positive sera were tested under optimized competitive ELISA conditions to assess method specificity. A PEDV-positive serum served as a control.

2.10. Comparison with commercial kits

101 serum samples were tested using the established competitive ELISA methods and commercial kits. The concordance rate between the two methods was calculated, and the compliance rate was expressed as: Compliance rate (%) = (number of negative sera detected similarly + number of positive sera detected similarly)/total serum number × 100 %.

3. Results

3.1. Identification of MNPs-N

The carboxyl groups on the MNPs reacted with the EDC and NHC solutions forming an activated ester solution. This solution reacts with the amino groups on the PEDV N protein forming the MNPs-N probe. TEM results(Fig. 2ab) revealed tiny protrusions on the surface of MNPs-N, indicating successful N protein attachment. Particle size analysis (Fig. 2c) revealed the average particle size of the original MNPs to be about 500 nm, and MNPS-N about 800 nm. MNPs-N had a significantly larger particle size compared to MNPs, indicating the successful preparation of the MNPs-N probe.

3.2. Identification of anti-N McAb and McAb-HRP probe

Tail tip blood serum was withdrawn from mice after two immunizations. The serum potency of the immunized mice was measured using indirect ELISA, with the serum diluted from 1:1000 to 1:2,048,000. The results indicated that the serum potency of the immunized mice reached a dilution of 1:2,048,000 (Fig. 3a). Positive mouse 2 was chosen for cell fusion to prepare monoclonal antibodies.

The McAb reactivity with N protein was assessed by Western blot (Fig. 3b) and IFA. The IFA results demonstrated that monoclonal antibodies produced specific fluorescence signals with the virus-attached

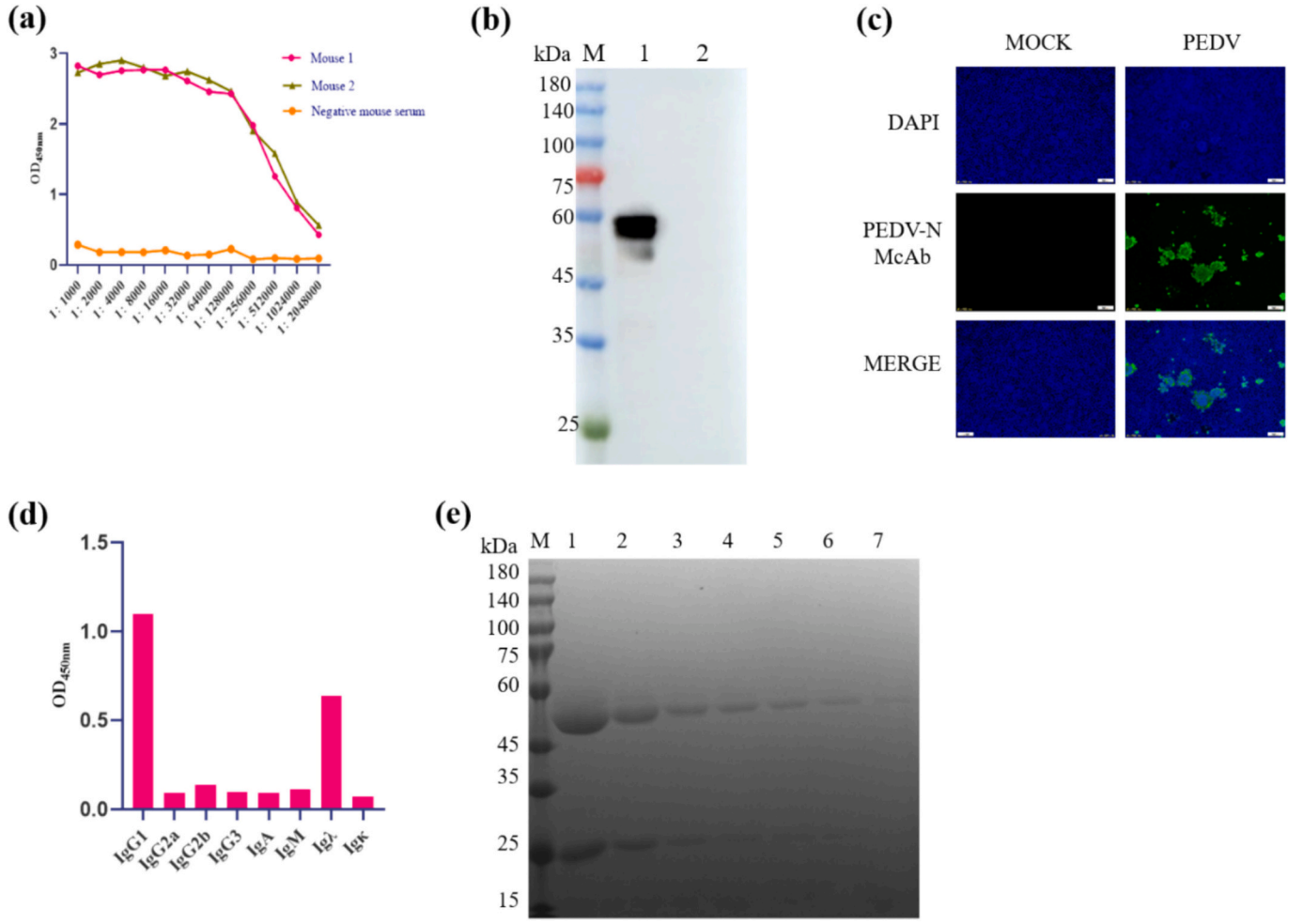

Fig. 3. Preparation and characterization of McAb. (a) Indirect ELISA for the detection of specific IgG titer in BALB/c mice. (b) Western blot results of the reaction with N protein McAb. Lane 1 was N protein, lane 2 was S protein negative control. (c) IFA identification. (d) Schematic diagram of McAb subtype identification. (e) SDS-Page electrophoresis results of the purified McAb. Lanes 1–7 are purified antibodies.

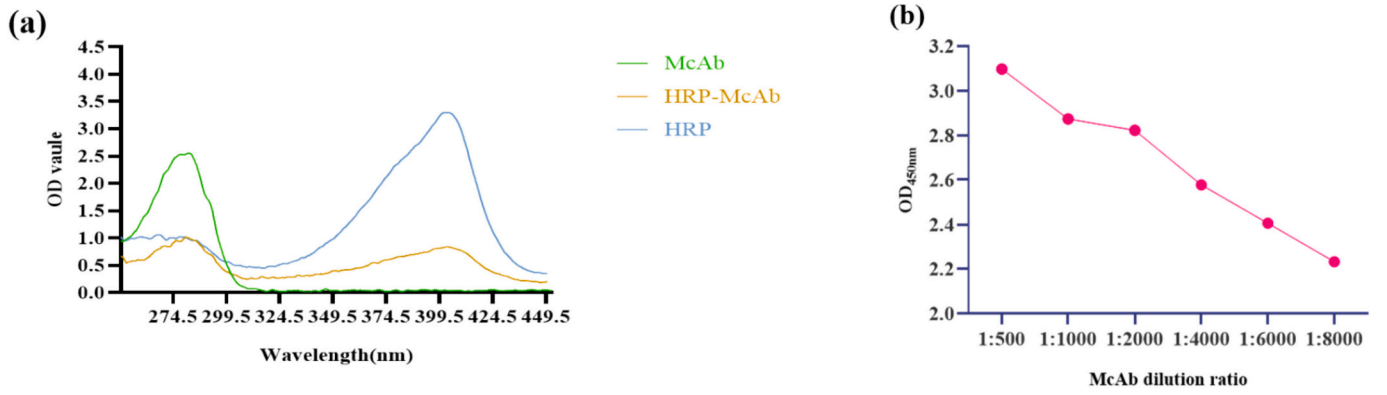

Fig. 4. Validation of the McAb-HRP probe. (a) UV–Vis scanning spectra of McAb-HRP. (b) ELISA detection of the McAb-HRP probe.

Vero cells, while the negative control did not exhibit fluorescence signals (Fig. 3c). The hybridoma cell supernatant (the primary antibody) was identified using the Triple Eagle Mouse Monoclonal Antibody Subtype Identification Kit. The monoclonal antibody subtype was identified as IgG1 with a Kappa chain (Fig. 3d). Ascites were prepared from hybridoma cells and purified (Fig. 3e). High-purity monoclonal antibodies against the N protein were obtained.

The synthesized McAb-HRP conjugate was identified using a UV spectrophotometer and direct ELISA. The absorption peak of McAb-HRP integrates the absorption peaks of McAb and HRP (Fig. 4a). Additionally, the activity of the McAb-HRP probe was assessed using ELISA. McAb within the synthesized probe maintains a high affinity for the N protein (Fig. 4b), indicating that the affinity of McAb for N protein or the catalytic ability of HRP remains unaffected.

Table 1
Determination of the optimal concentration of MNPs-N probe and the optimal dilution of McAb-HRP probe (PI).

MNPs-N concentration (μg/mL)	McAb-HRP dilution					
	1:500	1:1000	1:2000	1:4000	1:6000	1:8000
0.2	70.60 %	70.54 %	70.47 %	38.31 %	37.15 %	50.00 %
1	73.63 %	76.72 %	79.71 %	68.40 %	63.60 %	65.94 %
2	69.59 %	72.38 %	71.27 %	67.30 %	65.13 %	55.48 %
4	63.18 %	70.18 %	74.54 %	69.90 %	57.04 %	38.85 %
8	38.99 %	52.61 %	56.67 %	51.53 %	46.76 %	24.83 %

3.3. Competitive ELISA method condition optimization

The optimal concentrations of MNPs-N and McAb-HRP probes were determined using the checkerboard method. The MNPs-N probe was diluted in PBS solution to obtain five concentration gradients (0.2 μg/mL, 1 μg/mL, 2 μg/mL, 4 μg/mL, and 8 μg/mL). The McAb-HRP probe was serially diluted (1:500, 1:1000, 1: 2000, 1:4000, 1:6000, and 1:8000). The highest PI value was observed when the MNPs-N probe at 1 μg/mL and the McAb-HRP probe at 1:2000 dilution (Table 1).

A PEDV positive serum was serially diluted (undiluted, 1:1, 1:2, 1:5, 1:10, and 1:20) and tested. OD_{450} values reading revealed that undiluted serum had the highest PI value. Thus, no dilution was required for optimal performance (Fig. 5a). The optimal reaction time was found to be 30 min (Fig. 5b), and optimal color development duration was determined (Fig. 5c).

The final optimized assay conditions were a combination of 50 μL of undiluted serum, 50 μL of MNPs-N (1 μg/mL), and 50 μL of McAb-HRP

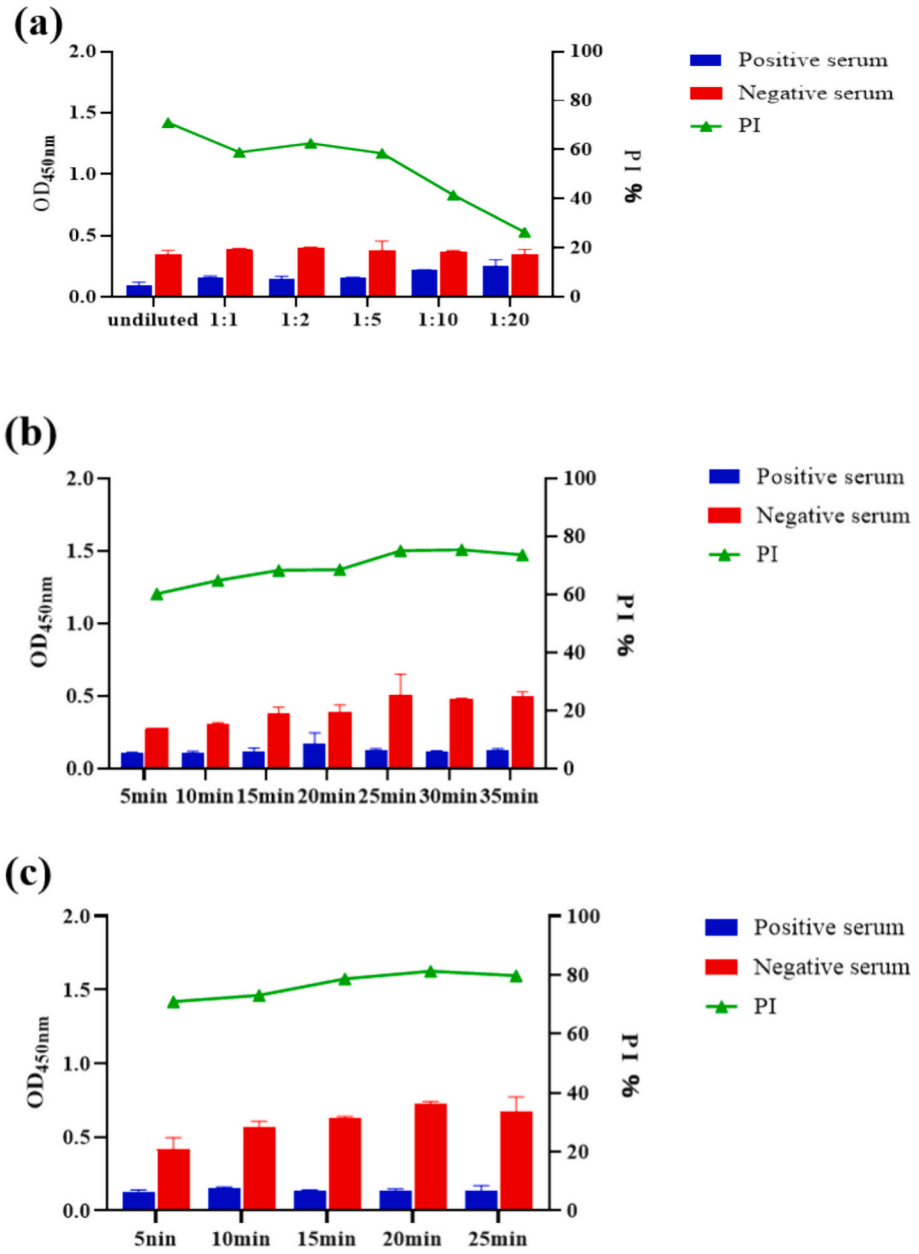

Fig. 5. Optimization results of the two-probe competitive ELISA method. (a) Determination of the optimal sample dilution ratio. (b) Determination of the optimal sample reaction time. (c) Determination of the optimal color development time.

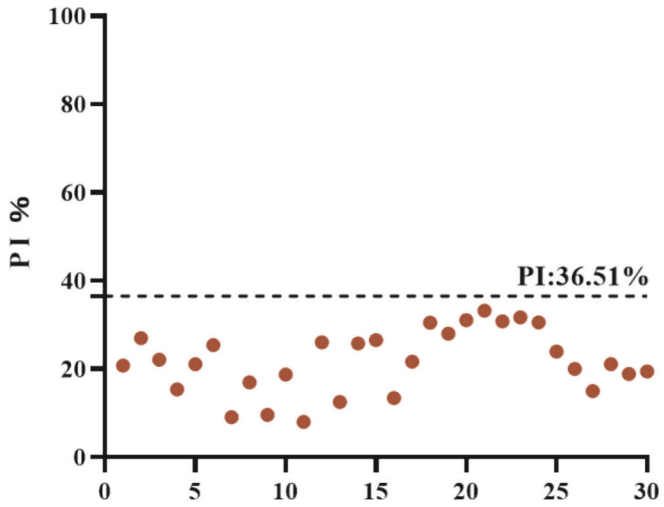

Fig. 6. Determination of the cut-off value.

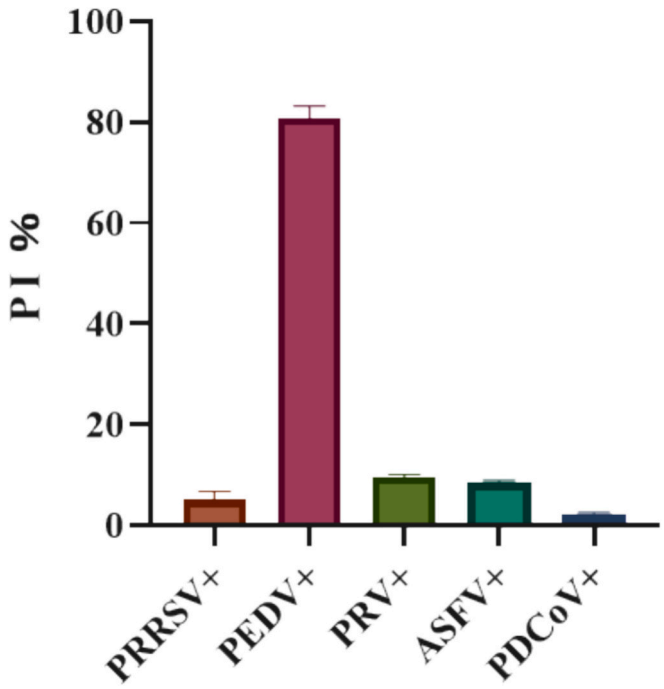

Fig. 7. Results of the specificity test.

Table 3
Clinical sample detection.

Clinical samples	Two-probe competitive ELISA method		Commercial Kits		Compliance rate (%)
	No. of negative	No. of positive	No. of negative	No. of positive	
101	22	79	15	86	93.07 %

diluted at a ratio of 1:2000. The reaction proceeded at room temperature for 30 min, followed by 20-min color development with TMB solution.

3.4. Determination of critical values

Optimized competitive ELISA was used to evaluate 30 PEDV-negative sera. The mean (X) sample inhibition rate was 21.83 %, and the standard deviation (SD) was 7.34 %. The result was considered negative if it was less than X + 2 SD = 36.51 %, positive if it was greater than X + 3 SD = 43.85 %, and doubtful if it was between 36.51 % and 43.85 % (Fig. 6).

3.5. Specificity and reproducibility tests

PRRSV-positive sera, PRV-positive sera, ASFV-positive sera, PDCoV-positive sera and PEDV-positive serum controls were used to assess the specificity of ELISA (Fig. 7). Good specificity was observed only for PEDV-positive seropositivity.

Optimized competitive ELISA was used to assess seven PEDV-positive sera. The intra- and inter-batch coefficients of variation were under 10 % (Table 2), indicating that the method was reproducible and stable.

3.6. Comparison with commercialized kits

ELISA was used to assess 101 serum samples stored in the laboratory, and the compliance rate with commercial kits was calculated. ELISA detected 79 positive sera and 22 negative sera, while the commercialized kit identified 86 positive sera and 15 negative sera. Thus, the compliance rate was 93.07 % (Table 3).

4. Discussion

During the early stages of the PED epidemic, the classical CV777 strain vaccine was effective. As mutants emerged after 2010, those previously vaccinated were also affected. This caused a critical concern within the pig industry. These variants increased piglet mortality rates to 80–100 % [8]. Currently, there are no medicines or vaccines available to control these outbreaks [37]. Current strategies focus on preventing virus introduction through infected animals and assessing vaccination efficacy in pregnant sows. Several diagnostic techniques are employed for detecting PED, including immunofluorescent antibody technology (IFA), immunohistochemistry, fluorescent quantitative PCR, and ELISA [38]. ELISA stood out for its analysis capacity. It could handle large

Table 2
Results of the repeatability test.

Sample no.	Inter-assay Intra-assay					
	X	SD	CV%	X	SD	CV%
1	0.775758336	0.044226158	5.70 %	0.789205658	0.015811386	2.00 %
2	0.765830519	0.01922436	2.51 %	0.782005575	0.023897687	3.06 %
3	0.510580611	0.050990773	9.99 %	0.521748486	0.048385868	9.27 %
4	0.815300401	0.02932812	3.60 %	0.790702079	0.030065915	3.80 %
5	0.687837363	0.033734311	4.90 %	0.706612876	0.052708275	7.46 %
6	0.70776853	0.013555886	1.91 %	0.71069568	0.024768722	3.48 %
7	0.677427353	0.038854693	5.73 %	0.646453104	0.056974719	8.81 %

sample volumes efficiently and could measure antibody titers in serum and colostrum, thereby assessing vaccination responses [39]. An indirect ELISA for the detection of PEDV serum developed by Yang et al. [40], an indirect ELISA targeting IgA antibodies by Wang et al. [41], and a novel double-antibody sandwich quantitative ELISA by Han et al. [42] are some recent advancements. All these methods have high sensitivity, specificity, and simplicity. Maternal antibodies could confer neonatal protection against PEDV, and monitoring sow antibody levels is imperative [43]. Although easy to use, traditional ELISA could be complex and require time.

MNPs offer a promising alternative, functioning as solid supports that facilitate rapid antigen-antibody binding *via* a magnetic field [44]. MNPs versatility extends to hormones [45], neurotransmitters [46], cytokines [47], and tumor-associated antigens [48] too. This feature enables more research to resolve the complicated and time-consuming operation of traditional ELISA. In this study, MNPs are used to enhance PED diagnostics.

The ELISA involved a 30-minute incubation with MNPs-N and McAb-HRP probes, followed by colorimetric analysis after washing. The wells were washed four times with PBST, and the color-developing solution was added. This was incubated for 20 min in the dark. OD_{450} value was read after adding the stop solution to determine if the samples were positive. The critical value was determined by evaluating 30 negative sera. The specificity and reproducibility were assessed and compared with commercial assay kits. The final results showed a 93.07 % compliance of the competitive ELISA with the kit. Due to its specific detection method, only positive sera PRRSV, PRV, PDCoV and ASFV were detected. Other porcine diarrhea diseases could not be detected, indicating the need for improvements in future tests. The intra- and inter-batch coefficients of variation were less than 10 %, indicating good reproducibility. The assay was completed in 50 min, faster than other traditional ELISA methods. This optimized competitive ELISA supports the epidemiological investigation, clinical diagnosis, and PED epidemic control.

Ethics stateme

The experimental animal research protocol was approved by the Animal Care and Utilization Committee of Henan Agricultural University (HNND2024121901).

CRediT authorship contribution statement

Junru Sun: Writing – original draft, Methodology, Investigation, Data curation. **Ruiqin Zhu:** Writing – review & editing, Visualization, Validation. **Mengxiang Wang:** Resources, Formal analysis. **Jinxing Song:** Resources, Formal analysis. **Lei Zhou:** Conceptualization. **Zhuoya Sun:** Conceptualization. **Yanze Li:** Software. **Liuyang Jiao:** Software. **Lu Xia:** Resources. **Hua He:** Resources. **Gaiping Zhang:** Supervision. **Yanan Wu:** Supervision.

Funding

This work was supported by the National Key Research and Development Program for Young Scientists (2022YFD1801400) and Major Science and Technology Special Programs of Henan Province (221100110600, 231111113100), as well as the Natural Science Foundation of Henan Province (222300420181).

Declaration of competing interest

The authors declare that there is no conflict of interest.

Acknowledgement

We thank Dr Xie Caihua from the Henan Animal Epidemic Control Centre for providing PDCOV-positive sera, and Professor Ma Shijie from Henan Agricultural University for providing PEDV-positive sera.

References

[1] Y. Qiu, Y. Sun, X. Zheng, L. Gong, L. Yang, B. Xiang, Identification of host proteins interacting with the E protein of porcine epidemic diarrhea virus, Front. Microbiol. 15 (2024) 1380578.
[2] M. Li, Y. Pan, Y. Xi, M. Wang, Q. Zeng, Insights and progress on epidemic characteristics, genotyping, and preventive measures of PEDV in China: a review, Microb. Pathog. 181 (2023) 106185.
[3] K. Zhang, S. Lin, J. Li, S. Deng, J. Zhang, S. Wang, Modulation of innate antiviral immune response by porcine enteric coronavirus, Front. Microbiol. 13 (2022) 845137.
[4] H. Yu, G. Chen, T. Zhang, X. Huang, Y. Lu, M. Li, S. Li, C. Wang, B. Li, Y. Zhang, G. Liu, Y. Fu, PEDV promotes the differentiation of CD4(+)T cells towards Th1, Tfh, and Treg cells via CD103(+) DCs, Virology 587 (2023) 109880.
[5] V.T. Than, S.E. Choe, T.T.H. Vu, T.D. Do, T.L. Nguyen, T.T.N. Bui, T.N. Mai, R. M. Cha, D. Song, D.J. An, V.P. Le, Genetic characterization of the spike gene of porcine epidemic diarrhea viruses (PEDVs) circulating in Vietnam from 2015 to 2016, Vet. Med. Sci. 6 (3) (2020) 535–542.
[6] M.B. Pensaert, P. Martelli, Porcine epidemic diarrhea: a retrospect from Europe and matters of debate, Virus Res. 226 (2016) 1–6.
[7] C. Lee, Porcine epidemic diarrhea virus: An emerging and re-emerging epizootic swine virus, Virol. J. 12 (2015) 193.
[8] J. Lei, Y. Miao, W. Bi, C. Xiang, W. Li, R. Zhang, Q. Li, Z. Yang, Porcine epidemic diarrhea virus: etiology, epidemiology, antigenicity, and control strategies in China, Animals (Basel) 14 (2) (2024).
[9] D.M. Kim, S.H. Moon, S.C. Kim, H.S. Cho, D. Tark, Genetic and pathogenic analysis of a novel porcine epidemic diarrhea virus strain isolated in the Republic of Korea, Viruses 16 (7) (2024).
[10] K. Yu, X. Liu, Y. Lu, M. Long, J. Bai, Q. Qin, X. Su, G. He, X. Mi, C. Yang, R. Wang, H. Wang, Y. Chen, Z. Wei, W. Huang, K. Ouyang, Biological characteristics and pathogenicity analysis of a low virulence G2a porcine epidemic diarrhea virus, Microbiol. Spectr. 11 (3) (2023) e0453522.
[11] F. Zhao, X.A. Ma, J. Yang, Z. Wei, J. Li, Y. Jiang, W. Cui, Z. Shan, L. Tang, Investigation of transmission and evolution of PEDV variants and co-infections in Northeast China from 2011 to 2022, Animals: an open access journal from MDPI 14 (15) (2024) 2168.
[12] F. Lin, H. Zhang, L. Li, Y. Yang, X. Zou, J. Chen, X. Tang, PEDV: insights and advances into types, function, structure, and receptor recognition, Viruses 14 (8) (2022).
[13] K. Jung, L.J. Saif, Q. Wang, Porcine epidemic diarrhea virus (PEDV): An update on etiology, transmission, pathogenesis, and prevention and control, Virus Res. 286 (2020) 198045.
[14] Z. Shi, J. Wu, Y. Zhu, J. Zhou, B. Hu, Effects of host proteins interacting with non-structural protein nsp9 of porcine epidemic diarrhea virus on viral replication, Sheng Wu Gong Cheng Xue Bao 39 (12) (2023) 4824–4836.
[15] S. Sungsuwan, A. Jongkaewwattana, P. Jaru-Ampornpan, Nucleocapsid proteins from other swine enteric coronaviruses differentially modulate PEDV replication, Virology 540 (2020) 45–56.
[16] Y. Zhao, B. Fan, J. Xue, R. Guo, J. Li, J. Zhou, X. Song, X. Zhang, S. Tao, B. Li, Characterization and epitope mapping of monoclonal antibodies against PEDV N protein, Virology 579 (2023) 29–37.
[17] M. Sun, Y. Sun, L. Zhang, Y. Gao, Z. Wang, X. Wang, P. Jiang, J. Bai, Identification and characterization of new B cell epitopes on the nucleocapsid protein of porcine epidemic diarrhea virus using monoclonal antibodies, Vet. Microbiol. 298 (2024) 110200.
[18] J. Zhou, C. Xue, Y. Hou, M. Li, Y. Hu, Q. Chen, Y. Li, K. Li, G. Song, K. Cai, Z. Luo, Oxygenated theranostic nanoplatforms with intracellular agglomeration behavior for improving the treatment efficacy of hypoxic tumors, Biomaterials 197 (2019) 129–145.
[19] F. Nadeem, F. Fozia, M. Aslam, I. Ahmad, S. Ahmad, R. Ullah, M.H. Almutairi, L. Aleya, M.M. Abdel-Daim, Characterization, antiplasmodial and cytotoxic activities of green synthesized Iron oxide nanoparticles using nephrolepis exaltata aqueous extract, Molecules 27 (15) (2022).
[20] S. Alavinia, R. Ghorbani-Vaghei, Magnetic Fe3O4 nanoparticles in melamine-based ternary deep eutectic solvent as a novel eco-compatible system for green synthesis of pyrido[2,3-d]pyrimidine derivatives, J. Mol. Struct. 1270 (2022) 133860.
[21] H. Poursadegh, M. Barzegarzadeh, M.S. Amini-Fazl, Preparation of pH-sensitive chitosan-magnetic graphene quantum dot bionanocomposite hydrogel beads for drug delivery application: emphasis on effects nanoparticles, Polyhedron 247 (2024) 116705.
[22] H. Poursadegh, M.S. Amini-Fazl, S. Javanbakht, F. Kazeminava, Magnetic nanocomposite through coating mannose-functionalized metal-organic framework with biopolymeric pectin hydrogel beads: a potential targeted anticancer oral delivery system, Int. J. Biol. Macromol. 254 (2024) 127702.
[23] F. Mollarasouli, E. Zor, G. Ozcelikay, S.A. Ozkan, Magnetic nanoparticles in developing electrochemical sensors for pharmaceutical and biomedical applications, Talanta 226 (2021) 122108.
[24] A.M. Azzam, M.A. Shenashen, M.S. Selim, B. Mostafa, A. Tawfik, S.A. El-Safty, Vancomycin-loaded furriness amino magnetic nanospheres for rapid detection of gram-positive water bacterial contamination, Nanomaterials (Basel) 12 (3) (2022).
[25] C. Das, S. Singh, S. Bhakta, P. Mishra, G. Biswas, Bio-modified magnetic nanoparticles with Terminalia arjuna bark extract for the removal of methylene

blue and lead (II) from simulated wastewater, Chemosphere 291 (Pt 2) (2022) 132673.
[26] G.T. Tee, X.Y. Gok, W.F. Yong, Adsorption of pollutants in wastewater via biosorbents, nanoparticles and magnetic biosorbents: a review, Environ. Res. 212 (Pt B) (2022) 113248.
[27] A. Avasthi, C. Caro, E. Pozo-Torres, M.P. Leal, M.L. García-Martín, Magnetic nanoparticles as MRI contrast agents, Top Curr. Chem. (Cham) 378 (3) (2020) 40.
[28] A. Gharehkhani, R. Ghorbani-Vaghei, S. Alavinia, Synthesis of calixresorcarenes using magnetic poly triazine-benzene sulfonamide-SO(3)H, RSC Adv. 11 (59) (2021) 37514–37527.
[29] R. Ghorbani-Vaghei, S. Alavinia, Z. Merati, V. Izadkhah, MNPs@SiO-Pr-AP: a new catalyst for the synthesis of 2-amino-4-aryl thiazole derivatives, Appl. Organomet. Chem. 32 (3) (2018).
[30] J.Y. Seo, S.B. Park, S.Y. Kim, G.J. Seo, H.K. Jang, T.J. Lee, Acoustic and magnetic stimuli-based three-dimensional cell culture platform for tissue engineering, Tissue Eng. Regen. Med. 20 (4) (2023) 563–580.
[31] A. Sadžak, M. Eraković, S. Šegota, Kinetics of flavonoid degradation and controlled release from functionalized magnetic nanoparticles, Mol. Pharm. 20 (10) (2023) 5148–5159.
[32] S. Mourdikoudis, A. Kostopoulou, A.P. LaGrow, Magnetic nanoparticle composites: synergistic effects and applications, Adv. Sci. (Weinh) 8 (12) (2021) 2004951.
[33] J. Hong, L. Wang, Q. Zheng, C. Cai, X. Yang, Z. Liao, The recent applications of magnetic nanoparticles in biomedical fields, Materials (Basel) 17 (12) (2024).
[34] S. Mallakpour, M. Tukhani, C.M. Hussain, Sustainable plant and microbes-mediated preparation of Fe(3)O(4) nanoparticles and industrial application of its chitosan, starch, cellulose, and dextrin-based nanocomposites as catalysts, Int. J. Biol. Macromol. 179 (2021) 429–447.
[35] C.P. Jia, X.Q. Zhong, B. Hua, M.Y. Liu, F.X. Jing, X.H. Lou, S.H. Yao, J.Q. Xiang, Q. H. Jin, J.L. Zhao, Nano-ELISA for highly sensitive protein detection, Biosens. Bioelectron. 24 (9) (2009) 2836–2841.
[36] S. Zhang, L. Wang, L. Wang, N. Yu, Y. Dong, J. Hu, Combined antibody tagged HRP gold nanoparticle probe for effective PCV2 screening in pig farms, Int. J. Nanomedicine 17 (2022) 3361–3369.
[37] Z. Li, Z. Ma, Y. Li, S. Gao, S. Xiao, Porcine epidemic diarrhea virus: molecular mechanisms of attenuation and vaccines, Microb. Pathog. 149 (2020) 104553.
[38] E.A. Flores-Contreras, J.A. Carrasco-González, D.C.L. Linhares, C.A. Corzo, J. I. Campos-Villalobos, A. Henao-Díaz, E.M. Melchor-Martínez, H.M.N. Iqbal, R. B. González-González, R. Parra-Saldívar, E. González-González, Emergent molecular techniques applied to the detection of porcine viruses, Vet. Sci. 10 (10) (2023).
[39] M. Olech, Current state of molecular and serological methods for detection of porcine epidemic diarrhea virus, Pathogens 11 (10) (2022).
[40] X. Yang, L. Li, X. Su, J. Li, J. Liao, J. Yang, Z. Xiao, P. Wen, H. Wang, Development of an indirect enzyme-linked immunosorbent assay based on the yeast-expressed CO-26K-equivalent epitope-containing antigen for detection of serum antibodies against porcine epidemic diarrhea virus, Viruses 15 (4) (2023).
[41] K. Wang, Z. Hu, M. Fan, Z. Shao, Q. Yu, X. Li, Development of an indirect ELISA to detect PEDV specific IgA antibody based on a PEDV epidemic strain, BMC Vet. Res. 18 (1) (2022) 319.
[42] W. Han, Z. Ma, Z. Li, C. Chang, Y. Yuan, Y. Li, R. Feng, C. Zheng, Z. Shi, H. Tian, H. Zheng, S. Xiao, A novel double antibody sandwich quantitative ELISA for detecting porcine epidemic diarrhea virus infection, Appl. Microbiol. Biotechnol. 108 (1) (2024) 482.
[43] X. Niu, Q. Wang, Prevention and control of porcine epidemic diarrhea: the development of recombination-resistant live attenuated vaccines, Viruses 14 (6) (2022).
[44] H. Tsai, Y.H. Lu, H.X. Liao, S.W. Wu, F.Y. Yu, C.B. Fuh, Detection of rabbit IgG by using functional magnetic particles and an enzyme-conjugated antibody with a homemade magnetic microplate, Chem. Cent. J. 9 (2015) 8.
[45] Q. Wei, P. Zhang, H. Pu, D.W. Sun, A fluorescence aptasensor based on carbon quantum dots and magnetic Fe(3)O(4) nanoparticles for highly sensitive detection of 17β-estradiol, Food Chem. 373 (Pt B) (2022) 131591.
[46] H.J. Cheon, Q.H. Nguyen, M.I. Kim, Highly sensitive fluorescent detection of acetylcholine based on the enhanced peroxidase-like activity of histidine coated magnetic nanoparticles, Nanomaterials (Basel) 11 (5) (2021).
[47] X. Wang, Z. Xia, H. Wang, D. Wang, T. Sun, E. Hossain, X. Pang, Y. Liu, Cell-membrane-coated nanoparticles for the fight against pathogenic bacteria, toxins, and inflammatory cytokines associated with sepsis, Theranostics 13 (10) (2023) 3224–3244.
[48] M. Roshani, A. Rezaian-Isfahni, M.H. Lotfalizadeh, N. Khassafi, M. Abadi, M. Nejati, Metal nanoparticles as a potential technique for the diagnosis and treatment of gastrointestinal cancer: a comprehensive review, Cancer Cell Int. 23 (1) (2023) 280.